

Novel Regulation of Aquaporins during Osmotic Stress¹

Rosario Vera-Estrella*, Bronwyn J. Barkla, Hans J. Bohnert, and Omar Pantoja

Departamento de Biología Molecular de Plantas, Instituto de Biotecnología, Universidad Nacional Autónoma de México, Cuernavaca, Morelos, 62250, México (R.V.-E., B.J.B., O.P.); and Departments of Plant Biology and Crop Sciences, University of Illinois, Urbana, Illinois 61801–3838 (H.J.B.)

Aquaporin protein regulation and redistribution in response to osmotic stress was investigated. Ice plant (*Mesembryanthemum crystallinum*) McTIP1;2 (McMIPF) mediated water flux when expressed in *Xenopus laevis* oocytes. Mannitol-induced water imbalance resulted in increased protein amounts in tonoplast fractions and a shift in protein distribution to other membrane fractions, suggesting aquaporin relocalization. Indirect immunofluorescence labeling also supports a change in membrane distribution for McTIP1;2 and the appearance of a unique compartment where McTIP1;2 is expressed. Mannitol-induced redistribution of McTIP1;2 was arrested by pretreatment with brefeldin A, wortmannin, and cytochalasin D, inhibitors of vesicle trafficking-related processes. Evidence suggests a role for glycosylation and involvement of a cAMP-dependent signaling pathway in McTIP1;2 redistribution. McTIP1;2 redistribution to endosomal compartments may be part of a homeostatic process to restore and maintain cellular osmolarity under osmotic-stress conditions.

It seems intuitively obvious that plant water channels, aquaporins (AQP), ought to play a dynamic role in maintaining cellular water homeostasis under conditions that necessitate modifications in water flux. Changes in water uptake and allocation would be required to balance alterations in the cellular osmotic potential and, therefore, AQP activity and/or expression should be tightly regulated.

Environmental stimuli, including drought, dehydration, desiccation, and salinity, as well as a rise in abscisic acid (ABA), which accompanies the perception of osmotic stress, have been shown to regulate the expression of both tonoplast (vacuolar membrane; TP) and plasma membrane (PM) AQP at the transcript level (for review, see Maurel et al., 2002).

Recent evidence supports a direct role for aquaporins in plant water relations and provides information on their involvement in drought stress tolerance. Manipulation of PM intrinsic protein (PIP) transcript levels through overexpression (Aharon et al., 2003), or through gene silencing by antisense suppression (Kaldenhoff et al., 1998; Martre et al., 2002; Siefritz et al., 2002) or T-DNA insertion (Javot et al., 2003), resulted in changes in root hydraulic conductivity, transpiration rates, and cellular osmotic water potential and, in some cases, directly affected the plant's ability to recover from water deficit conditions (Martre et al., 2002; Siefritz et al., 2002; Aharon et al., 2003).

Few studies have addressed the direct regulation of AQP expression by osmotic stress at the protein level, and fewer still have focused on AQP dynamic behavior. However, when factors such as mRNA stability and, conceivably, altered turnover under stress conditions are considered, evidence for transcriptional regulation may be less compelling than observations indicating that protein amounts are directly affected.

In the ice plant (*Mesembryanthemum crystallinum*), regulation of AQP protein amount by salinity stress was observed using peptide-specific antibodies. McTIP1;2 amounts in leaf TP decreased during salt stress and levels of McPIP2;1 (McMIPC) in root PM fractions were induced, while McPIP1;4 (McMIPA) showed no change (Kirch et al., 2000). For McTIP1;2, the decrease in protein amount in the presence of NaCl was contrasted by an increase in the presence of mannitol (Vera-Estrella et al., 2000), suggesting precise deciphering and discrimination of osmotic and ionic signaling pathways.

Little is known about the synthesis of AQP and the pathway delivering them to their destination membranes. Endosomal trafficking of plant AQP may play a role in the regulation and turnover of these proteins at their target membrane under conditions of osmotic stress. In animals, regulatory cycling between membranes has been demonstrated for several AQP. Vasopressin-induced increases in water permeability of kidney-collecting duct cells have been shown to occur via shuttling of AQP2 from intracellular vesicles to the apical PM through exocytosis (Nielsen et al., 1995; for review, see Knepper and Inoue, 1997). Also, acetylcholine-induced increases in cytoplasmic Ca²⁺ appeared to trigger the translocation of AQP5 from intracellular membranes to the apical PM of rat parotid tissue (Ishikawa et al., 1999). In the ice plant, changes in membrane distribution of the TP AQP McTIP1;2, correlated with changes in osmotic potential,

¹ This work was supported by the Consejo Nacional de Ciencia y Tecnología (grant nos. 31794N to R.V.-E. and 33054N to O.P.) and by the National Science Foundation International Program (USA-Mexico; to O.P. and H.J.B.).

* Corresponding author; e-mail rosario@ibt.unam.mx; fax 777-3114691.

Article, publication date, and citation information can be found at www.plantphysiol.org/cgi/doi/10.1104/pp.104.044891.

have been suggested (Barkla et al., 1999) and observed (Vera-Estrella et al., 2000). Here, we further characterize regulation of the ice plant AQP *McTIP1;2* under osmotic stress, and begin to dissect the mechanisms responsible for the stress-induced changes in *McTIP1;2* membrane distribution.

RESULTS

Ice Plant *McTIP1;2* Is a Functional Water Channel in *Xenopus* Oocytes

To study and begin to physiologically interpret the changes in abundance and distribution of *McTIP1;2* from the ice plant exposed to osmotic stress, it was important to functionally characterize the protein in more detail. We used expression studies in *Xenopus* oocytes to determine if *McTIP1;2* could indeed mediate water transport. Oocytes expressing *McTIP1;2* showed a 37-fold increase in swelling rate compared to oocytes injected with ribonuclease (RNase)-free water (Fig. 1A). Included as a positive control were oocytes expressing *AtTIP1;1*, which characteristically exhibits high water permeability in oocytes (Maurel et al., 1993). *McTIP1;2* showed comparable rates of swelling as *AtTIP1;1*-injected oocytes (Fig. 1A). Based on the rate of swelling and the imposed osmotic gradient, we calculated the osmotic water permeability (P_f) for oocytes expressing *McTIP1;2* and *AtTIP1;1* and compared these values to the P_f calculated from water-injected oocytes (Fig. 1B). *McTIP1;2*-injected oocytes had a calculated P_f of $13.9 \times 10^{-3} \text{ cm s}^{-1}$, 11-fold higher than that of the water-injected oocytes and a value close to the P_f calculated for *AtTIP1;1* expressed in oocytes ($15.0 \times 10^{-3} \text{ cm s}^{-1}$; Fig. 1B). These values indicated that *McTIP1;2* facilitated the transport of water. Whether or not it is strictly selective for water requires further study.

Ice Plant *McTIP1;2* Is Differentially Regulated by Salt and Osmotic Stress

Previous results with peptide-specific antibodies had suggested a complex regulation of *McTIP1;2* (Kirch et al., 2000; Vera-Estrella et al., 2000). Extending these studies, we have observed that *McTIP1;2* is slightly down-regulated by salt (200 mM) and up-regulated by mannitol (200 mM), sorbitol (200 mM), and ABA (25 μM ; Fig. 2; Vera-Estrella et al., 2000). Under osmotic-stress conditions, in addition to the 34-kD band, a second polypeptide of 41 kD appeared that cross-reacted with the *McTIP1;2* antibody, possibly a glycosylated form of *McTIP1;2* (see below).

Membrane Distribution of *McTIP1;2* Is Altered by Osmotic Stress

Suc density gradient separation of microsomal membranes from untreated cell suspensions showed that *McTIP1;2* cofractionated with markers for the TP

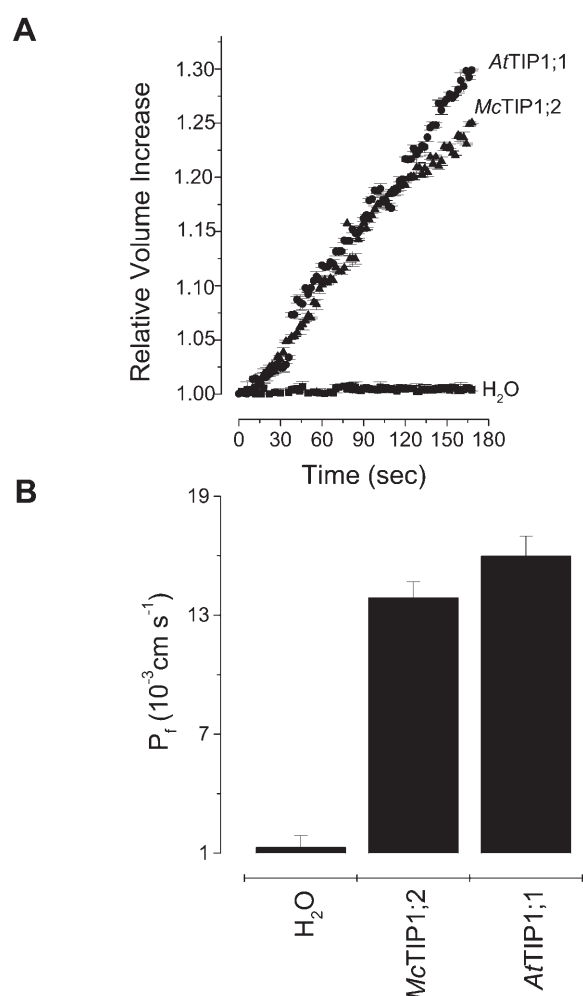


Figure 1. Water permeability of *McTIP1;2* and *AtTIP1;1* expressed in *Xenopus* oocytes. A, Time courses of changes in the relative volume increases of *Xenopus* oocytes injected with 50 ng of the indicated cRNA or RNase-free water. The relative volume increases were measured with reference to initial volume (set as 1) and plotted as a function of time after the introduction of oocytes into 40 mosmol kg⁻¹ hypotonic saline solution at time zero. B, P_f values calculated from the initial rate of oocyte swelling as described in "Materials and Methods." Values are the mean \pm SE ($n = 10$).

(highest expression in fractions 16–25, corresponding to 13%–20% Suc; Fig. 3, A, B, and G). However, under osmotic stress (mannitol, Fig. 3, A and B; sorbitol or ABA; data not shown), *McTIP1;2* amounts in TP fractions increased, and it was also detected in fractions that overlapped with Golgi (UDPase activity; Fig. 3F), endoplasmic reticulum (ER; calreticulin and cytochrome-c reductase activity; Fig. 3, A, C, and F), prevacuolar compartments (PVC; Pep12; Fig. 3, A and D; Sanderfoot et al., 1998), and the vacuolar-sorting receptor, BP80, that traffics between clathrin-coated vesicles, Golgi, and PVC (Fig. 3, A and E; Paris et al., 1997). Interestingly, in the presence of mannitol, BP80 expression also increased (Fig. 3, A and E). The peak of *McTIP1;2* expression was shifted to fractions 25 to 31

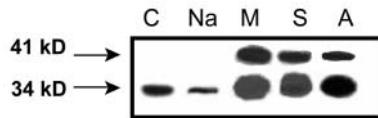


Figure 2. Differential expression of *McTIP1;2* under salt, osmotic, or ABA treatment in TP fractions of ice plant cell suspensions. Cells were incubated for 5 d with 200 mM of either NaCl (Na), mannitol (M), sorbitol (S), or 25 μ M ABA (A) before isolation of TP on a discontinuous Suc density gradient at the 0/16% (w/v) Suc interface. Blots are representative of five independent experiments.

(20%–23% Suc), which overlapped closely to the peak for Golgi markers (Fig. 3, A, B, and F).

Differences in the response of *McTIP1;2* to salt and osmotic stress (Figs. 2 and 3A, *McTIP1;2*-M and -S) suggest that the ionic component of the salt stress initiates a separate and independent signaling pathway resulting in a decrease in expression of the *McTIP1;2* protein, while osmotic stress, in the absence of an ionic signal, results in the up-regulation and apparent redistribution of *McTIP1;2*.

Indirect immunofluorescence microscopy of living cells gave a clearer picture of *McTIP1;2* redistribution under osmotic stress. In control cells the fluorescence associated with *McTIP1;2* recognition was present only in the TP (Fig. 4A, *McTIP1;2*-C), showing a similar distribution to that observed for the TP V-PPase (Fig. 4A, V-PPase). Upon mannitol treatment, *McTIP1;2*-associated fluorescence was altered and could be seen in the cytosol, possibly associated with vesicles (Fig. 4A, *McTIP1;2*-M), but not associated with the PM (Fig. 4A, *McHKT1*-M). This distribution was similar to that observed for BP80, in control (not shown) and mannitol-treated cells (Fig. 4A, BP80-M), and for Pep12 (data not shown), confirming results obtained from the Suc density gradient separation of membranes (Fig. 3). This mannitol-induced membrane distribution was unique for *McTIP1;2* as no alterations were observed for P-ATPase, V-PPase, *McHKT1*; PEP12, *AfTIP2;1*, and calreticulin (Fig. 3, A and B; Fig. 4, A and B; data not shown).

Double-labeling of cells with *McTIP1;2* and BP80 antibodies allowed us to define the relationship between the structures carrying both antigens. As observed in Figure 4B, *McTIP1;2* and BP80 do not appear to colocalize in control cells as *McTIP1;2* primarily labeled the TP, and BP80, cytosolic structures (Fig. 4B, control). In cells treated with mannitol, partial colocalization of *McTIP1;2* and BP80 is indicated as observed by the merging of colors in the cytosol (Fig. 4B, mannitol). However, *McTIP1;2* was the only antigen that labeled the spherical vesicular compartments present in mannitol-treated cells (Fig. 4B, mannitol [arrows]). We have so far been unable to determine the origin of this compartment as it does not label with any of the available markers, including TP (V-PPase, V-ATPase), PM (P-ATPase, *McHKT1*), protein storage vacuoles (PSV; *AfTIP2;1*), and PVC (BP80 and Pep12; Fig. 4B; data not shown).

McTIP1;2 Membrane Redistribution Is Organ Specific and Temporally Regulated

Changes in *McTIP1;2* similar to those observed in suspension cells (Fig. 5, cells) were also observed in membranes from leaves of osmotically stressed plants (Fig. 5, leaves). Whereas membranes from roots showed a mannitol-induced increase in *McTIP1;2* amounts in TP fractions, no change in membrane distribution or appearance of the 41-kD polypeptide was observed (Fig. 5, roots). This contrasting response suggests that the mannitol-induced redistribution of *McTIP1;2* in the leaves is organ specific and controlled, and not primarily due to an accumulation of newly synthesized proteins in membranes.

To further investigate mechanisms involved in regulating the distribution of *McTIP1;2* during osmotic stress, we determined the time course of the observed changes. Modifications in protein amount and membrane distribution were observed within 2 h of exposure to 200 mM mannitol (Fig. 6A), while increases in mRNA levels were observed only in the first h of mannitol treatment (Fig. 6B) and then remained at a steady level. Over time, *McTIP1;2* protein amounts were seen to increase in heavier fractions (peak observed in fraction 22), while levels in fraction 13, corresponding to TP, initially increased but subsequently decreased (Fig. 6A). These data suggest that the redistribution of *McTIP1;2* is due to posttranslational regulation and not the further synthesis of mRNA or protein.

The 41-kD Polypeptide Is a Glycosylated Form of *McTIP1;2*

In addition to the observed changes in protein amount and the changes in membrane distribution of *McTIP1;2* upon mannitol treatment, the appearance of a 41-kD protein that also cross-reacted with the *McTIP1;2* antibody was observed (Figs. 2, 3, 5, and 6 A). The possibility that this second immunoreactive polypeptide was a glycosylated form of *McTIP1;2* was investigated. Membrane fractions collected from continuous Suc gradients were immunoprecipitated with the anti-*McTIP1;2* antibody, separated by SDS-PAGE, transferred onto nitrocellulose membranes, and subsequently stained for the detection of both N-linked and O-linked oligosaccharides (see "Materials and Methods"). Under control conditions, no glycosylation of the 34-kD *McTIP1;2* was detected (Fig. 7A, ProQ Fuchsia); however, immunoprecipitated fractions from the mannitol-treated cells showed glycosylation of the 41-kD polypeptide in all fractions in which the protein was detected (Fig. 7B, ProQ Fuchsia). Treatment with tunicamycin, which blocks the formation of N-glycosidic protein carbohydrate linkages, was able to block both the membrane redistribution of *McTIP1;2* and the appearance of the 41-kD glycoprotein (Fig. 7B, *McTIP1;2* and ProQ Fuchsia + tunicamycin). In contrast, tunicamycin had no effect on the TP location of *McTIP1;2* in the control-treated cells (Fig. 7A,

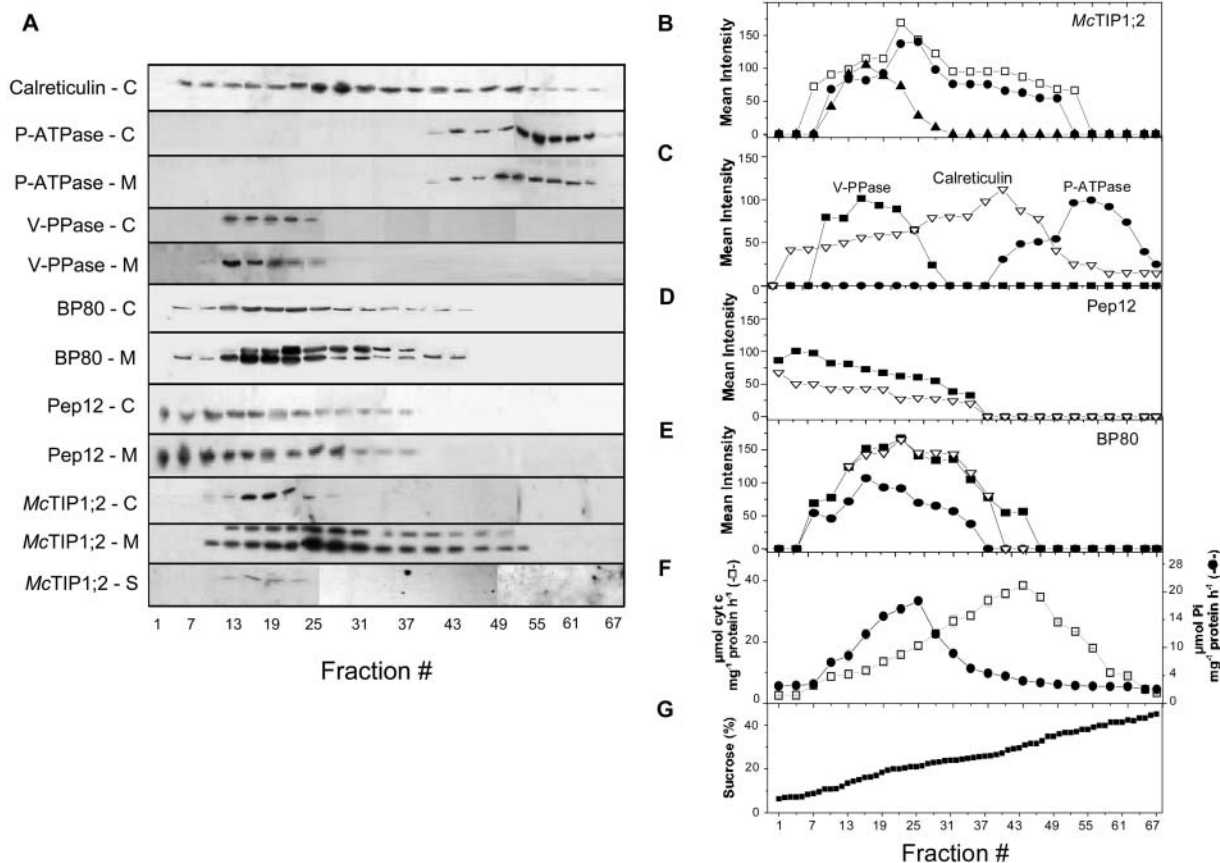


Figure 3. Expression of *McTIP1;2* and marker enzyme colocalization under mannitol stress. Western-blot analysis of microsomal fractions from ice plant cell suspensions. Individual blots (eight lanes/blot) were digitally photographed (Kodak DC-120; Kodak, Mexico City), and then images were aligned and joined using the imaging software PhotolImpact SE 3.01 (Ulead Systems, Torrance, CA) in order to enable visualization of all representative fractions. A, Immunological detection in the respective fractions of (from top to bottom), calreticulin (57 kD), P-ATPase (PMA-1; 100 kD), V-PPase (PAB-HK; 70 kD), BP80 (80 and 85 kD), Pep12 (37 kD), *McTIP1;2* (34 kD and 41 kD); C, control, M, mannitol, or S, salt treatment. B, Mean intensity of the bands from *McTIP1;2*-control (▲), and *McTIP1;2*-mannitol (●, 41 kD and □, 34 kD)-treated microsomal fractions. C, Mean intensity of the immunolocalized markers (▽) calreticulin, (●) P-ATPase, (■) V-PPase in microsomal fractions. D, Mean intensity of the immunolocalized marker Pep12 in control (●) and mannitol-treated (■) microsomal fractions. E, Mean intensity of the immunolocalized marker BP80 in control (●) and mannitol-treated (■, 80 kD and ▽, 85 kD) microsomal fractions. F, Distribution of marker enzyme-specific activity in microsomal fractions. (□) NADH cytochrome c reductase and (●) UDPase. G, Suc concentrations in collected fractions. The blots are representative of at least four independent experiments.

McTIP1;2 + tunicamycin). We have also observed that the distribution and expression of V-ATPase, P-ATPase, *McHKT1*, BP80, and calreticulin did not change upon tunicamycin treatment (data not shown).

McTIP1;2 Membrane Redistribution Is the Result of Complex Signaling Mechanisms

To decipher mechanisms involved in the changes in *McTIP1;2* membrane distribution induced by osmotic stress, we used brefeldin A (BFA), a specific inhibitor that causes disassembly of Golgi complexes and disruption of vesicular trafficking in eukaryotes (Chardin and McCormick, 1999; Ritzenthaler et al., 2002). Pre-incubation of cells with BFA (10 $\mu\text{g}/\text{mL}$) for 30 min was sufficient to inhibit both the increase in *McTIP1;2* protein in the TP fractions and the mannitol-induced

membrane redistribution of the AQP (Fig. 8B). The inhibition of osmotic stress-induced protein increases could indicate that BFA inhibited the trafficking of *McTIP1;2* between membranes and affected protein synthesis and the normal targeting and delivery of proteins to their resident membranes. To investigate this possibility, we followed the expression of marker enzymes under the same treatment. The presence of BFA did not affect protein levels or distribution of the V-ATPase (VHA-E; E-subunit) or P-ATPase (PMA1), markers for the TP and PM, respectively, pointing to a specific effect of BFA on *McTIP1;2* trafficking (Fig. 8). Further evidence that this was not a general effect on protein synthesis was obtained by comparing the effects of BFA with those of the protein synthesis inhibitor cycloheximide. Pretreatment with cycloheximide for 30 min, followed by 2 h mannitol treatment,

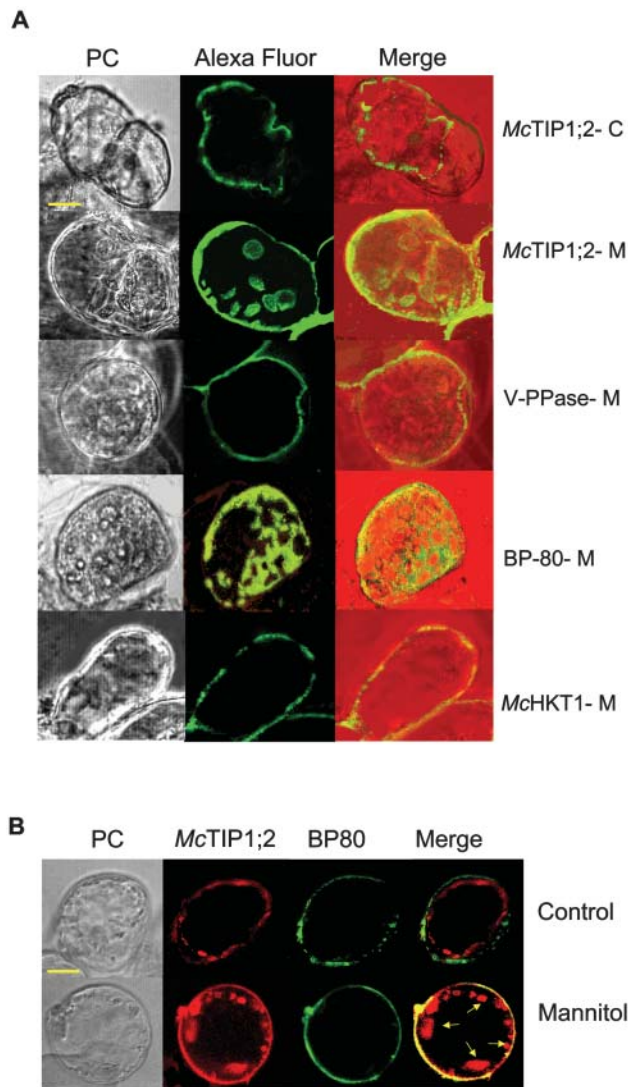


Figure 4. Indirect immunofluorescent labeling of mannitol-treated ice plant cells. **A**, Cell suspensions were grown for 5 d and then incubated for 5 h in the absence (*McTIP1;2*-C) or presence of 200 mM mannitol (*McTIP1;2*-M; V-PPase [PAB-HK]; BP80; *McHKT1*). Cells were prepared as described in “Materials and Methods” for immunolocalization. Cells were immunolabeled with anti-*McTIP1;2* antibodies (*McTIP1;2*-C and *McTIP1;2*-M) or antibodies directed against specific membrane markers: V-PPase as a marker for TP; BP80 as a marker of PVC; and *McHKT1* as a marker for PM, followed by labeling with the Alexa fluor 568 secondary antibody. On the merged images Alexa fluor 568 immunofluorescence is shown in green and the phase contrast image (PC) appears in red. **B**, Double labeling of ice plant cells with *McTIP1;2* and BP80. Cells were prepared as described in “Materials and Methods” for immunolocalization. Control and mannitol-treated cells were labeled with *McTIP1;2* and BP80. On the merged images *McTIP1;2* is shown in red, BP80 in green, the colocalization of both proteins in yellow, and the vesicular compartments are indicated by arrows. The images are representative of at least four independent experiments. Bar, 50 μm .

did not result in changes to protein amount. More importantly, redistribution of *McTIP1;2* and the V-ATPase or P-ATPase markers was not affected by the presence of this protein synthesis inhibitor. (Fig. 9A; data not shown).

Pulse chase labeling experiments followed by immunoprecipitation of total protein also confirmed that the redistribution of *McTIP1;2* was not due to normal trafficking to the TP of newly synthesized *McTIP1;2*. Met labeling of the 34-kD *McTIP1;2* protein was observed after 30 min incubation with mannitol, and no further increase in protein synthesis was detected after this time. Rather there was a decrease in the amount of 34-kD *McTIP1;2* protein with the subsequent appearance of the 41-kD glycosylated form of *McTIP1;2* (Fig. 9B). No Met labeling of the 41-kD glycosylated form of *McTIP1;2* was observed in cells incubated in the absence of mannitol (Fig. 9B).

Spatial and temporal regulation of membrane budding, movement, and fusion can be achieved by localized, rapid changes in phosphoinositide levels through the action of protein kinases and phosphatases (Simonsen et al., 2001). One of these,

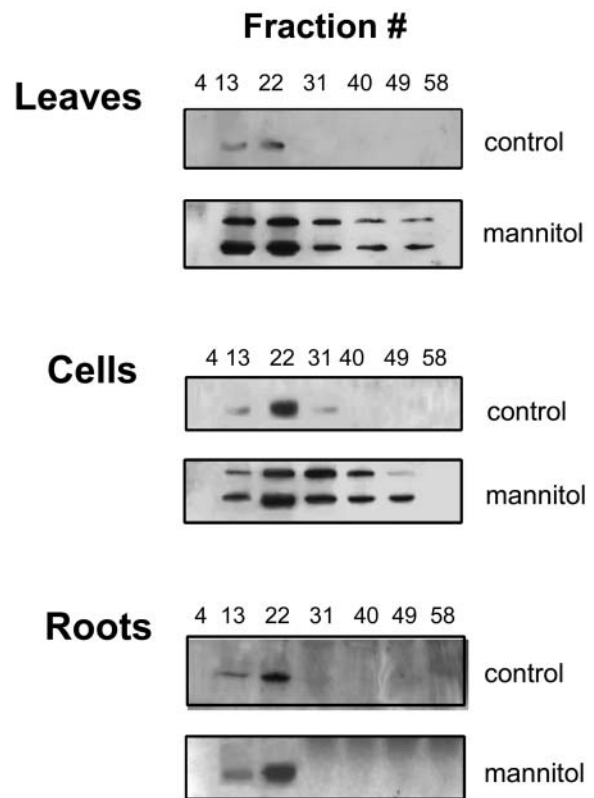


Figure 5. *McTIP1;2* membrane redistribution is tissue specific. Roots and leaves were obtained from plants grown in hydroponic culture 5 d after addition of 200 mM mannitol. Cell suspension cultures were treated for 5 h with 200 mM mannitol. Microsomal membranes from control, salt-, or mannitol-treated cell suspensions (cells), leaves, and roots were separated on continuous Suc density gradients. The blots are representative of at least four independent experiments.

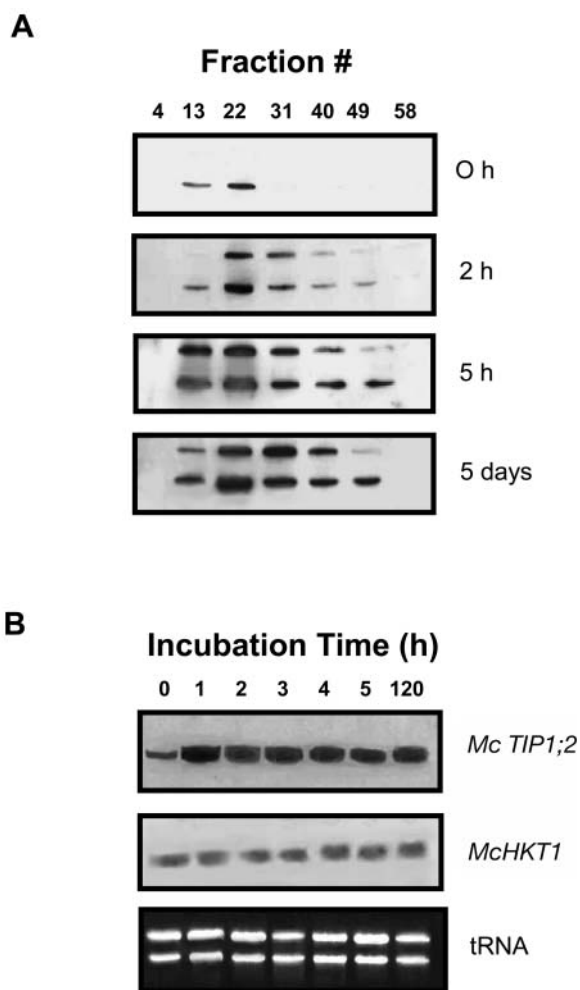


Figure 6. Time dependence of mannitol-induced changes in *McTIP1;2* synthesis and protein redistribution. Ice plant cells were grown for 5 d and then incubated for the indicated times with 200 mM mannitol. A, Microsomal fractions were isolated and separated on continuous Suc density gradients. Protein samples were separated by 12.5% SDS-PAGE, transferred to nitrocellulose membranes, and probed with anti-*McTIP1;2* antibodies. B, RNA gel-blot analysis of *McTIP1;2* and *McHKT1* transcripts (1,250 and 1,907 nucleotides, respectively) hybridized to total RNA from cell suspensions treated with 200 mM mannitol for the times indicated. Ethidium bromide stained gel (bottom) shows equal RNA loading prior to blotting. Blots are representative of three independent experiments.

phosphatidylinositol 3-phosphate kinase, plays a role in regulating the availability of phosphatidylinositol 3-phosphate. Changes in the level of phosphatidylinositol 3-phosphate can disrupt endocytic membrane trafficking (Simonsen et al., 2001). Wortmannin, a specific inhibitor of phosphatidylinositol 3-phosphate kinase (Woscholski et al., 1994), disrupted the mannitol-induced changes in *McTIP1;2* distribution; *McTIP1;2* was exclusively detected in fractions associated with TP (Fig. 10, wortmannin). Disruption of cytoskeletal components, including microtubules or actin microfilaments, can also affect membrane trafficking.

Cytochalasin D-induced depolymerization of actin filaments significantly inhibited *McTIP1;2* membrane redistribution under osmotic stress (Fig. 10, cytochalasin D); however, the *McTIP1;2* 34-kD polypeptide and the 41-kD glycopeptide were still detected in fractions coinciding with TP markers.

In animals, the translocation of AQP2-laden intracellular vesicles to the apical PM is triggered by vasopressin binding to an adenylyl cyclase (AC)-V₂ coupled receptor, resulting in an increased level of cAMP, which subsequently activates cAMP-dependent protein kinase A (PKA). PKA phosphorylation of AQP2 regulates delivery of the protein to the apical PM (Brown et al., 1998). Sequence analysis of ice plant *McTIP1;2* identified a possible PKA phosphorylation site motif at the N terminal of the protein (positions 4–7). The possibility that similar signaling molecules to those regulating AQP2 in animals may be involved in controlling *McTIP1;2* membrane redistribution was investigated. Treatment with forskolin, an activator of AC, known to elicit cAMP-dependent physiological responses by increasing intracellular cAMP (Hanoune and Defer, 2001), and 8-Br cAMP, a cell permeable cAMP analog that activates PKA (Baumgarten et al., 1998), in the absence of mannitol treatment mimicked and enhanced the effect of mannitol-induced osmotic stress on *McTIP1;2* membrane redistribution (Fig. 10, forskolin and 8-Br cAMP). In contrast, pretreatment with 2',5'-dideoxyadenosine (2,5-D), an inhibitor of AC (Hanoune and Defer, 2001), prior to mannitol exposure appeared to restrict the *McTIP1;2* protein to TP fractions on the Suc gradient with no protein detected in fractions of higher density (Fig. 10, 2,5-D). Direct inhibition of PKA by the specific inhibitor H89 prevented the redistribution of *McTIP1;2* protein (Fig. 10, H89).

DISCUSSION

Heterologous expression of AQP in *Xenopus* oocytes has provided substantial information toward functional characterization of these proteins. A number of plant AQP are permeable to water to varying degrees. *Arabidopsis AtTIP1;1*, belonging to the tonoplast intrinsic protein (TIP) subfamily, exhibits one of the highest P_f values of those characterized (Maurel et al., 1993). *McTIP1;2*, which also belongs to this family, has similarly high water permeability (Fig. 1B). However, preliminary data indicate that *McTIP1;2* does not transport Na⁺, nitrate, or Zn⁺ but appears to be permeable to K⁺ (data not shown). This may support a role for this AQP in osmotic adjustment in plant cells.

Osmotic stress-induced increases in *McTIP1;2* protein amount were accompanied by rapid and prolonged changes in AQP membrane distribution (Figs. 3A, 4, A and B, and 5). These observations suggested involvement of membrane trafficking in the posttranslational control of *McTIP1;2* and presented evidence

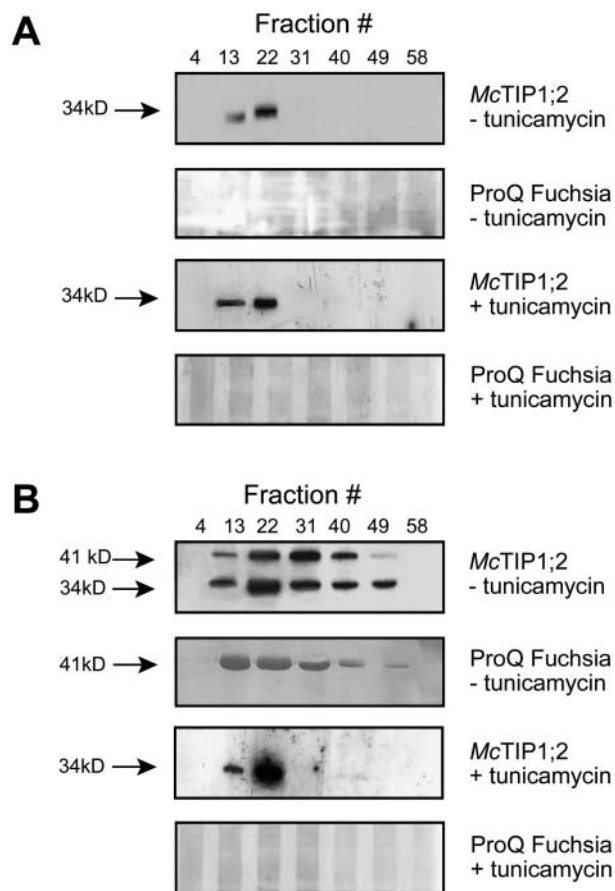


Figure 7. Glycosylation of *McTIP1;2* in mannitol-treated cells is necessary for membrane redistribution. Microsomal proteins from control (A) or mannitol-treated (B) cells were layered onto continuous Suc density gradients, and fractions were either prepared directly for SDS-PAGE or immunoprecipitated with the anti-*McTIP1;2* antibodies as described in "Materials and Methods." Samples were then resuspended in Laemmli (1970) sample buffer, separated by SDS-PAGE, and transferred to nitrocellulose membranes. Blots of SDS-PAGE-separated microsomal proteins were used for immunological detection of *McTIP1;2* (*McTIP1;2* $-/+$ tunicamycin) as described in "Materials and Methods." Blots of immunoprecipitated protein were used for glycoprotein staining with the ProQ Fuchsia kit (ProQ Fuchsia $-/+$ tunicamycin) as described in "Materials and Methods". Tunicamycin (25 μ M) was added to cells 30 min prior to the 12-h incubation period in the absence or presence of mannitol. Blots are representative of three independent experiments.

for a novel mechanism in the regulation of AQP activity under stress conditions in plants.

Membrane trafficking between different compartments, including ER, Golgi, TP, and PM can follow a number of routes. Aside from the TP of large central vegetative vacuoles, AQP belonging to the TIP subfamily, which includes *McTIP1;2*, have been shown to reside on membranes of other vesicles, including PSV, lytic vesicles, autophagic vacuoles, and electron-dense vesicles (Jauh et al., 1999). It appears that these TIP denote their respective compartments in a developmentally preprogrammed sense with a specific TIP de-

fining a particular vacuole type, although it is also possible to detect more than one TIP colocalized to the same membrane (Jauh et al., 1999). The complexity increases with the evidence that different stages of vacuole biogenesis and different types of vacuolar compartments can be present in a single cell type and changes can be triggered by environmental conditions (Paris et al., 1996; Marty, 1999). Vesiculation has also been reported to occur in animal cells as a means to prevent cytosolic dilution (Hazelton et al., 2001). Evidence also supports several independent pathways for the biogenesis and maintenance of vacuoles (Jiang and Rogers, 1998; Chrispeels and Herman, 2000). *McTIP1;2* could reside on a novel vacuole-type compartment that is induced by mannitol stress. Support for this view comes from electron microscopy analyses that showed the appearance of multivesicular bodies in the cytoplasm of mannitol-treated cells (data not shown). The location of *McTIP1;2* to a different membrane may help to maintain osmotic balance within the cytoplasm during the stress-induced uptake of specific solutes or ions into these vesicles. The Arabidopsis AQP/PIP1;1 has been shown to reside on plasmalemmasomes, endosomal vesicles thought to arise as a result of PM invaginations, whose physiological significance is unknown (Robinson et al., 1996). While the corn (*Zea mays*) *ZmPIP1b-sGFP* transgene expressed in tobacco (*Nicotiana tabacum*) is localized to the PM and the perinuclear region, suggesting that this PIP may be targeted to organelles involved in a secretory pathway (Chaumont et al., 2000). The *McTIP1;2*-associated compartments in this study may also be part of an extensive and complex endomembrane system capable of segmenting and inserting membranes where needed at the onset of the osmotic-stress response (Hazelton et al., 2001).

Vesicular trafficking of proteins involves a complex system that ensures the correct sequence of events leading to the final step of docking of the protein with its target membrane. Any signal transduction pathway that would relay the information and trigger relocation of the proteins will add another level of complexity. Disrupting components involved in protein sorting and targeting provided a way for deciphering the pathway involved in the redistribution of *McTIP1;2*. While transport of *McTIP1;2* (and other markers) to the TP was unaffected by BFA, a complete inhibition of the mannitol-induced redistribution of *McTIP1;2* was observed (Fig. 8). Previous results have already shown that the sorting of TIPs to the TP is insensitive to BFA (Gomez and Chrispeels, 1993). This indicates that the osmotic stress-induced redistribution of *McTIP1;2* follows a route that is independent of the normal delivery of this protein to the TP and, moreover, that it is BFA sensitive. This further suggests the requirement for independent functional vesicular sorting machinery involved in protein targeting to other endomembranes under osmotic-stress conditions. *McTIP1;2* redistribution under osmotic stress was also specifically perturbed by the presence of wortmannin (Fig. 10),

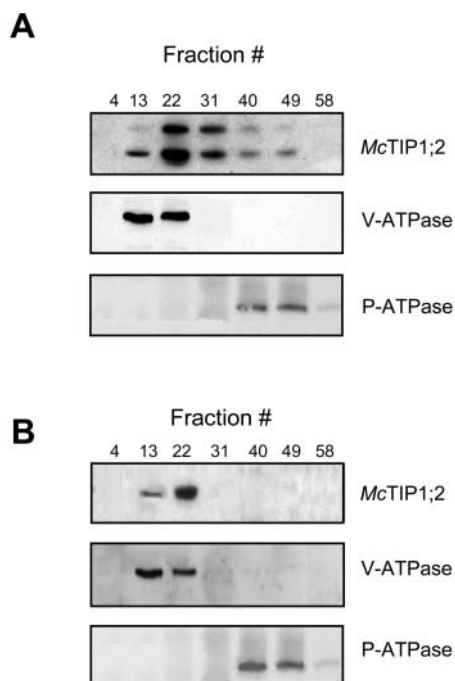


Figure 8. BFA inhibits the changes in *McTIP1;2* membrane distribution induced by mannitol treatment of ice plant cells. Microsomal fractions of ice plant cell suspensions were separated on continuous Suc density gradients and probed with antibodies for (from top to bottom) *McTIP1;2*, V-ATPase E-subunit (VHA-E), and P-ATPase (PMA1). A, Cells incubated with 200 mM mannitol for 2 h. B, Cells incubated for 30 min with 10 μg/mL BFA prior to incubation with 200 mM mannitol for 2 h. Blots are representative of five independent experiments.

providing further evidence for two independent pathways involved in *McTIP1;2* delivery to the TP and *McTIP1;2* trafficking under osmotic stress. Matsuoka et al. (1995) demonstrated, using wortmannin, the existence of distinct routes for sorting of soluble proteins to the vacuole, distinguished by their relative sensitivities to wortmannin. While we do not suggest that these pathways might direct *McTIP1;2*, our results indicate that phosphoinositide regulation of vesicular organization can show specificity for subsets of transport vesicles.

Disassembly of the actin cytoskeleton by cytochalasin D disrupted the redistribution of *McTIP1;2* under osmotic stress (Fig. 10), but not the appearance of the 41-kD polypeptide, suggesting that even though the glycosylated form is present, a functional cytoskeleton is essential for redistribution. This in part resembles vesicular trafficking of mammalian AQP2 and AQP5, which has been shown to be dependent on actin microfilaments and microtubules driving the sorting of the AQP-containing vesicles to their target membrane (Brown et al., 1998; Ishikawa et al., 1999). Moreover, AQP2 directly binds to actin *in vitro*, and drugs that disrupt cytoskeletal tracks have long been known to inhibit the hormonally induced change in permeability of the apical PM of renal epithelial cells (Brown

et al., 1998; Ishikawa et al., 1999). Rearrangement of the actin network occurs after hormonal exposure in these cells (Brown et al., 1998). In *Chara*, the specific sensitivity of endo-osmotic water flow to cytochalasins B and E provided early evidence for actin-mediated events that may be involved in regulating the localization and/or activity of plant AQP under certain conditions (Wayne and Tazawa, 1988).

cAMP-regulated signaling has been widely established in both eukaryotes and prokaryotes; however, the acceptance of its role in plants has been contentious, with only recent compelling evidence provided by more sensitive and accurate detection techniques (for review, see Newton et al., 1999) and the cloning of a putative AC in pollen, which shows homology to fungal ACs (Moutinho et al., 2001). Participation of a cAMP-signaling pathway in the redistribution of *McTIP1;2* under osmotic stress is suggested by our results. Inhibition of either cAMP synthesis or PKA activity, by 2,5-D, and H89, respectively, prevented *McTIP1;2* redistribution (Fig. 10). In contrast, stimulation of the pathway by either exogenous activation of

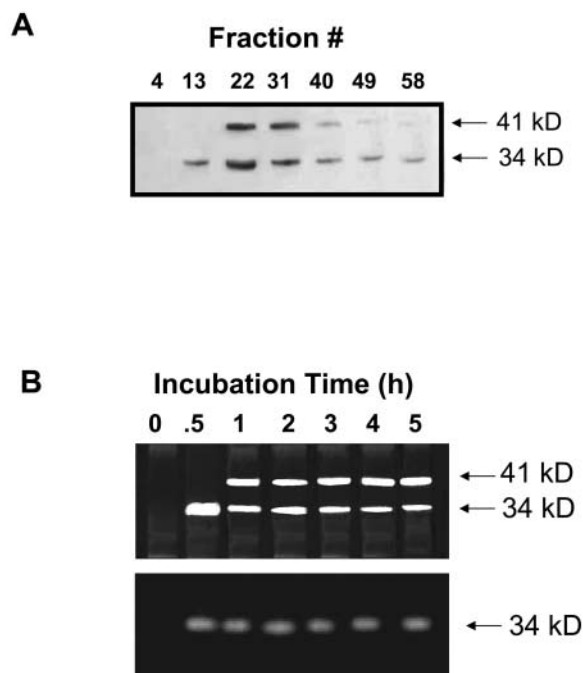


Figure 9. The redistribution of *McTIP1;2* is not a general effect of protein synthesis. A, Microsomal proteins from cells treated for 30 min with cycloheximide followed by 2 h with 200 mM mannitol treatment were isolated and separated on continuous Suc density gradients. The blot is representative of three independent experiments. B, *In vivo* pulse-chase labeling with ³⁵S Met/Cys for 1 h followed by incubation with (upper blot) or without (lower blot) 200 mM mannitol and by a chase with unlabeled Met and Cys for an additional 0.5 to 5 h. At the end of the pulse or chase equal amounts of cells were collected. Time zero refers to sampling of cells before the addition of Met. Total cell protein was extracted, immunoprecipitated with anti-*McTIP1;2* antibodies, and proteins separated on a 12.5% SDS-PAGE gel. Labeled proteins were detected with a PhosphorImager.

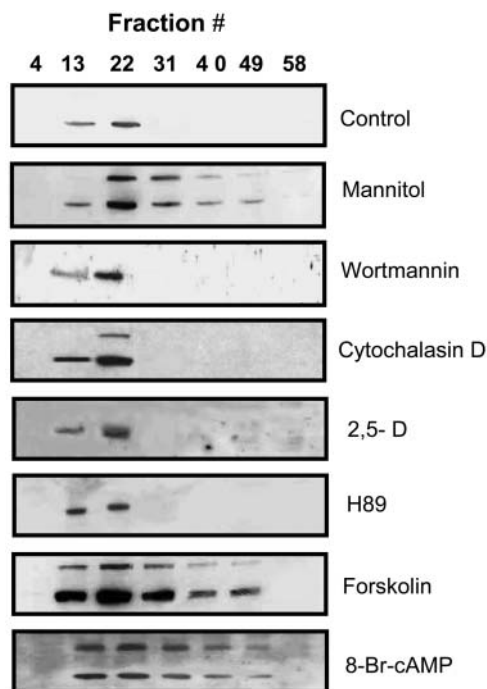


Figure 10. Mannitol-induced changes in membrane distribution of *McTIP1;2* is the result of complex signaling mechanisms. Ice plant cells were preincubated in the presence of either 10 nM wortmannin, 1.5 μ M cytochalasin D, 6 μ M 2,5-D, or 48 nM H89 for 30 min, followed by a 2-h incubation with 200 mM mannitol (blots 3–6). Ice plant cells incubated for 2 h with either 8 μ M forskolin or 40 μ M 8-bromoadenosine-3',5'-cyclic-monophosphate (8-Br cAMP) in the absence of mannitol treatment (blots 7 and 8). Untreated cells (control, blot 1) and cells treated for 2 h with 200 mM mannitol (mannitol, blot 2) were included as controls. Blots are representative of four independent experiments.

an AC (forskolin) or the use of a cAMP analog (8-Br cAMP) in the absence of mannitol treatment mimicked the osmotically induced changes in *McTIP1;2* distribution (Fig. 10). A role for cAMP signaling has previously been postulated for activation via phosphorylation of a plant AQP. Animal PKA was shown to phosphorylate *PvTIP3;1* (α -TIP) from kidney bean (*Phaseolus vulgaris*) in vitro, and increases in cAMP brought about by extrinsic activation of AC specifically increased the water transport activity of *PvTIP3;1* when expressed in *Xenopus* oocytes (Maurel et al., 1995). However, from these results it could not be decided whether phosphorylation by PKA directly affected the gating of the channel or, alternatively, enhanced targeting of the AQP to the membrane.

Two putative *N*-linked glycosylation sites are present in *McTIP1;2*. The motifs, NISG and NISL, are located at positions 78 to 81 and 97 to 100, respectively, which correspond to cytosolic loops. It appears that glycosylation is essential for *McTIP1;2* redistribution under mannitol treatment as inhibition of glycosylation blocks both the redistribution of the 34-kD *McTIP1;2* polypeptide and the appearance of the 41-kD glycopeptide (Fig. 7B, *McTIP1;2* + tunicamycin).

In eukaryotes, it has been suggested that *N*-linked oligosaccharides contain specific targeting information, and in plants, they have been shown to influence conformation, stability, and biological activity of proteins (Lerouge et al., 1998). Once the glycosylated form of *McTIP1;2* is localized to the new compartments, it appears to be deglycosylated, as both the glycosylated and nonglycosylated forms are observed in fractions from the mannitol-treated cells (Fig. 7B).

It has been reported that tunicamycin may cause the misfolding of glycoproteins. However, many reports have established that this drug has no effect on the folding of a large number of glycoproteins and does not affect the folding of nonglycosylated proteins (Cerioti et al., 1998). According to Sparvoli et al. (2000), tunicamycin treatment can affect plant glycoproteins in different ways depending upon the protein and the cell type involved. In our case, if *McTIP1;2* misfolding was occurring as a result of tunicamycin treatment, we would expect an increase of this protein in fractions corresponding to ER as a consequence of their retention and accumulation in this organelle. This should be clearly visualized using western-blot analyses of microsomal proteins after tunicamycin treatment. However, the fractions which correspond to ER (Fig. 7B; fractions 31–40) show no such accumulation of the 34-kD protein or any other protein that could represent the deglycosylated form of the 41-kD glycoprotein, if it is not *McTIP1;2*, but another AQP isoform (Fig. 7B). Rather, we see an increase in the unglycosylated *McTIP1;2* 34-kD polypeptide in the TP-associated fractions.

The existence of water channels has challenged views about plant water relations (Tyerman et al., 1999), but the large size of the AQP protein family may be even more puzzling (Santoni et al., 2000; Chaumont et al., 2001; Quigley et al., 2002). Judged by family size, apparently, plants need AQP in many membranes, or in different tissues in a complex pattern, or at different times under different external conditions. While we know that they transport water only from oocyte experiments, the list of metabolites that pass through AQP is growing (Tyerman et al., 2002; Liu et al., 2003; Uehlein et al., 2003). The complexity of AQP expression, from the control of transcript amount to post-translational modification by phosphorylation and glycosylation, is beginning to emerge. We add another component, the redistribution of a TP AQP depending on environmental conditions, to the list of mechanisms that guide the presence and functioning of AQP. The exact nature of the compartment to which *McTIP1;2* is redistributed upon mannitol treatment (Fig. 4, A and B) is still unclear, due to the complexity of vacuolar pathways in plant cells. However, our results indicate that upon mannitol treatment, *McTIP1;2* may reside in several membrane compartments (including a BP80-labeled compartment and a unique multi-vesicular compartment; Fig. 4, A and B) and that *McTIP1;2* redistribution depends on posttranslational modifications including glycosylation.

MATERIALS AND METHODS

Plant Materials and Growth Conditions

Ice plant (*Mesembryanthemum crystallinum*) plants and cell suspensions were grown as previously described (Barkla et al., 1999; Vera-Estrella et al., 1999). Cells were grown for 5 d following transfer to fresh Murashige and Skoog-supplemented medium (Murashige and Skoog, 1962) before treatment with 200 mM NaCl, or 200 mM mannitol or sorbitol, or 25 μ M ABA. Treatments were added to the existing cell medium as sterile crystals and/or powders to avoid changes in volume. Cells incubated in the presence of agonists and/or antagonists were observed microscopically for possible cellular damage, and cells were used only under conditions where cell viability was not affected.

Membrane Isolation and Purification

Membranes were isolated from ice plant plants and cell suspension cultures as previously described (Barkla et al., 1999; Vera-Estrella et al., 1999). Microsomes were layered onto either continuous (5% to 46% [w/v] Suc) or discontinuous Suc gradients (consisting of a top layer of 9 mL of 16% or 22% [w/v] Suc, over 9 mL of 32% [w/v] Suc, on a cushion of 9 mL of 38% [w/v] Suc). Gradients were centrifuged at 100,000g (3 h at 4°C) using a Beckman SW 28 swinging bucket rotor in a Beckman L8-M ultracentrifuge (Beckman, Mexico City). On a discontinuous Suc gradient TP from cell suspension cultures separates at the 0/16% Suc interface while PM is collected from the 32%/38% Suc interface (Vera-Estrella et al., 1999). TP isolated from root and leaf tissue is collected at the 0%/22% Suc interface (Barkla et al., 1999). The purity of the TP fraction was calculated by assaying for the relative contribution of PM, TP, and mitochondrial ATPase enzyme activities. From these studies it is estimated that the 0%/16% Suc interface had 85% bafilomycin and nitrate-sensitive ATPase activity (attributed to V-ATPase activity on the TP). No mitochondrial marker activity was detected (data not shown). Bands from the discontinuous gradient or fractions (0.5 mL) from the continuous Suc gradient were collected, frozen in liquid N₂, and stored at -80°C. The Suc concentration of fractions from continuous gradients was measured using a Zeiss refractometer (Zeiss, Mexico City). Previously we have shown that ice plant cell suspensions show similar adaptive responses as those of leaves to salt and osmotic stress (Vera-Estrella et al., 1999).

Pulse-Chase Labeling and Extraction of Total Protein

Cells of ice plant labeled for 1 h with ³⁵S Met/Cys followed by incubation from 0.5 to 5 h in the presence of 200 mM mannitol, were filtered onto Whatman Number 1 filter paper, frozen in liquid N₂, homogenized in extraction buffer (100 mM Tris-MES, pH 8.0, 1 mM EGTA, 5 mM dithiothreitol, 4 mM MgSO₄, 5% [w/v] insoluble PVP), and vortexed for 1 min. The samples were then filtered through one layer of Miracloth (Calbiochem, La Jolla, CA), and the crude protein extracts were centrifuged at 10,000g for 15 min using a SS34 rotor in a Sorvall 5C high speed centrifuge (DuPont, Newton, CT) to remove cellular debris. Samples were used for immunoprecipitation (see below) and resolved by SDS-PAGE on 12.5% (w/v) linear acrylamide gels. Signals were detected with a PhosphorImager (ImageQuant, Molecular Dynamics, Sunnyvale, CA).

Preparation of Template DNA, In Vitro Transcription, and Capping of mRNA

The coding region of *McTIP1;2* was cloned into the pGEM-HE vector, while *AfTIP1;1*, provided by Dr. C. Maurel, was cloned into the χ βG-ev2 vector (Maurel et al., 1993). Vectors contained either a T7 RNA polymerase promoter (pGEM-HE) or a T3 RNA polymerase promoter (χ βG-ev2), and 5'- and 3'- untranslated region of the *Xenopus laevis* β -globin gene for enhanced expression. The plasmid DNA was purified by polyethylene glycol precipitation and digested with either PstI (pGEM-HE) or XbaI (χ βG-ev2) that cleave immediately downstream of the inserts to produce a linear template. The linearized DNA was extracted with phenol-chloroform, precipitated with ethanol, and resuspended in RNase free water. The complementary RNAs (cRNAs) were synthesized in vitro using the mCAP(TM) mRNA capping kit (Stratagene, LaJolla, CA).

Oocyte Expression

Oocytes injected with 50 ng of cRNA were used 2 to 5 d post injection. The osmotic permeability of oocytes was measured by assaying the rates of oocyte

swelling upon rapid dilution from iso-osmotic Barth's solution [10 mM HEPES-NaOH, pH 7.4, 88 mM NaCl, 1 mM KCl, 2.4 mM NaHCO₃, 0.33 mM Ca(NO₃)₂, 0.41 mM CaCl₂, 0.82 mM MgSO₄, 200 mosmol/kg] to hypoosmotic dilute Barth's solution (40 mosmol/kg). Swelling was measured by video imaging on a Nikon Eclipse TE 300 microscope (Nikon, Mexico City), equipped with a Hitachi KP-D50 color video camera (Hitachi Denshi, Woodbury, NY). Images were captured and digitized by the Image-Pro Plus software (Version 4, Media Cybernetics, Silver Spring, MD).

The osmotic water permeability (P_f , cm/s) was calculated by the relation,

$$P_f = \frac{V_0(d[V/V_0]/dt)}{SV_w(osm_i - osm_o)}$$

where V_0 is the initial oocyte volume at time zero measured for each individual oocyte, V/V_0 is the relative volume, V_w is the partial molar volume of water (18 cm³/mol), S is the initial oocyte surface area calculated for each individual oocyte, osm_i is the osmolarity inside the oocyte, and osm_o is the osmolarity in the external medium. The time interval used for the calculations of P_f was 0 to 60 s.

Enzyme Assays

NADH cytochrome c reductase was measured spectrophotometrically at 25°C by following the reduction of cytochrome c at 550 nm as described (Hodges and Leonard, 1974). UDPase activity was measured in a 0.5 mL reaction volume containing 30 mM Tris/MES pH 7.3, 3 mM UDP-Tris, 3 mM MnSO₄ in the presence of 0.3% Triton X-100. Release of Pi was detected at 820 nm following the precipitation of Triton X-100 with TCA and HClO₄ (Manolson et al., 1985). Spectrophotometric measurements were taken using a diode array spectrophotometer (Hewlett-Packard, Mexico City).

Protein Determination

Protein content in microsomal and purified PM or TP fractions was measured by a modification of the dye-binding method of Bradford (1976), in which membrane protein was solubilized by the addition of 0.5% (v/v) Triton X-100 for 5 min before the addition of the dye reagent concentrate (Bio-Rad, Cuernavaca, Mexico).

Primary and Secondary Antibodies

A peptide representing the carboxy terminus of the deduced amino acid sequence of the ice plant *McTIP1;2* was synthesized, coupled to keyhole limpet hemocyanin, and antibodies were generated as previously described (Kirch et al., 2000). Anti-*McTIP1;2* was used at a dilution of 1:500. Antibodies against the V-ATPase E-subunit (VMA-E) from barley (*Hordeum vulgare*), V-Pase (PAB-HK) from sugar beet (*Beta vulgaris*), and the P-ATPase (PMA1) from Arabidopsis were kindly supplied by K.-J. Dietz, P.A. Rea, and R. Serrano, respectively (Pardo and Serrano, 1989; Kim et al., 1994; Dietz and Arbing, 1996). Antibodies against BP80 were kindly supplied by J.C. Rogers (Jauh et al., 1999). Calreticulin antibodies used were against the protein from Arabidopsis (Nelson et al., 1997). Pep12 monoclonal antibodies were purchased from Molecular Probes (Eugene, OR). Immunoconplexes were detected using a 1/5,000 dilution of either peroxidase labeled goat anti-mouse IgG secondary antibodies (BP80 and PEP12) or goat anti-rabbit IgG secondary antibodies (for detection of all other primary antibodies), and developed using the chemiluminescent ECL detection substrate (Amersham, Cuernavaca, Mexico). Film exposure time was kept constant for all blots.

Immunoprecipitation

Protein (30 μ g) was incubated with 500 μ L of NET-gel buffer (50 mM Tris/HCl, pH 7.5, 150 mM NaCl, 0.1% Nonidet P-40, 1 mM EDTA, and 0.25% gelatin) containing anti-*McTIP1;2* antibodies (1/500 dilution) for 1 h at 4°C on a rotating table. Protein A Sepharose CL-4B (20 μ L; Amersham Pharmacia Biotech, Uppsala) was added and the slurry rocked for a further 2 h at 4°C. Samples were then centrifuged at 12,000g for 20 s and the supernatant eliminated using a 1-mL syringe. The protein pellet was washed twice with NET-gel buffer followed by a final rinse with wash buffer (10 mM Tris/HCl, pH 7.5, 0.1% Nonidet P-40). The pellet was then resuspended with 20 μ L of 2.5%-Laemmli sample buffer (Laemmli, 1970), and heated at 95°C for 3 min.

Samples were centrifuged at 10,000g prior to loading onto a 12.5%-linear acrylamide gel for SDS-PAGE and subsequent protein blotting.

SDS-PAGE and Protein Immunoblotting

Samples were prepared according to the method of Parry et al. (1989). Protein was precipitated by dilution of the samples 50-fold in 1:1 (v/v) ethanol:acetone and incubated overnight at -30°C . Samples were then centrifuged at 13,000g for 20 min at 4°C using an F2402 rotor in a GS-15R table-top centrifuge (Beckman). Pellets were air dried, resuspended with Laemmli (1970) sample buffer (2.5% SDS final concentration), and heated at 60°C for 2 min before loading onto 12.5%-(w/v) linear acrylamide mini-gels. Unless stated in the figure legends, 12 μg of protein was loaded per lane. After electrophoresis, the gels were either stained with Coomassie Brilliant Blue R250 (0.25% [w/v] in 50% [v/v] methanol/7% [v/v] acetic-acid), destained in 10% methanol/10% acetic-acid (v/v), and dried under vacuum at 80°C for 2 h, or prepared for immunoblotting. SDS-PAGE-separated proteins were electrophoretically transferred onto nitrocellulose membranes (ECL, Amersham, Buckinghamshire, UK) as previously described (Vera-Estrella et al., 1999). Following transfer, proteins were stained with Ponceau S protein stain (0.1% w/v in 1% v/v acetic acid for 30 s) to check for equal loading/transfer of proteins. Membranes were then blocked with TBS (100 mM Tris, 150 mM NaCl) containing 0.02% (w/v) Na-azide, and 5% (w/v) fat-free milk powder for 2 h at room temperature. Blocked membranes were incubated for a minimum of 3 h at room temperature with the appropriate primary antibodies, followed by the addition of a 1:5,000 dilution of secondary antibodies (goat anti-rabbit or -mouse) conjugated to horse radish (*Armoracia lappathifolia*) peroxidase. Immunodetection was carried out using the chemiluminescent ECL western-blotting analysis system (Amersham, UK). Mean intensity of the immunodetected protein bands was calculated using ECL M_r markers as loading control standards (Amersham, Mexico). Images were captured using Kodak 1D image analysis software (Eastman Kodak, Rochester, NY).

Staining of Glycoproteins

In-blot staining of glycoproteins was performed using the Pro-Q fuchsia glycoprotein staining kit (Molecular Probes, Eugene, OR) according to manufacturer's instructions. Tunicamycin (25 μM) was added to cells 30 min prior to the 12 h incubation period in the presence or absence of mannitol.

Immunofluorescence

Cells were treated for 5 h with 200 mM mannitol and prepared for immunolabeling according to Brown and Lemmon (1995) with some modifications. Cells were fixed by incubation for 15 min at room temperature with 1.4% paraformaldehyde in stabilizing buffer containing 10 mM Bis-Tris propane, 25 mM HEPES, 2 mM MgCl_2 , 10 mM EGTA, pH 6.8. For control cells all solutions were adjusted to 200 mosmoles kg^{-1} , while solutions for mannitol-treated cells were adjusted to 500 mosmoles kg^{-1} . Fixed cells were then washed three times and cell walls were partially removed with an enzymatic cocktail (10 mM KCl, 2 mM MgCl_2 , 1 mM CaCl_2 , 10 mM ascorbic acid, 10 mM MES, 0.05% BSA [w/v], 1% cellulase [w/v], 0.02% [w/v] pectolyase, pH 6.8) for 20 min at room temperature. Following digestion, cells were washed and permeabilized with 1% Triton X-100 (v/v) in stabilizing buffer for 10 min with respective washes. Triton X-100 treatment also served to eliminate autofluorescence. Before addition of the primary antibodies the cells were incubated for 1 h with 0.5% (w/v) fat-free milk powder. Primary antibodies were added at a 1:100 dilution and all cells were incubated overnight at 4°C with gentle shaking, followed by addition of goat anti-rabbit or anti-mouse secondary Alexa fluor 568 antibodies (Molecular Probes) for 2 h at room temperature. For double-labeling experiments, cells were incubated sequentially with the primary antibody, followed by a mix of the corresponding secondary antibodies coupled to different fluorochromes (Alexa Fluor 488 or 568). The cells were imaged with a Bio-Rad Confocal laser microimager (Bio-Rad, Hercules, CA) mounted on a Carl Zeiss Axioskop fitted with a Neo-Fluar 40X/0.74 objective and using Cosmos 7.0 Software (Bio-Rad). The stored digital images were pseudo-colored as red or green images, using Photoshop 3.0 (Adobe, Mountain View, CA). For double-labeled cells, the separate images were pseudocolored, one as red, the other one as green, and then overlaid and/or merged using the confocal assistance software (Bio-Rad). This resulted in regions of colocalization appearing as yellow. To enable comparison, all images were recorded using the same parameters of laser power and photo-

multiplier sensitivity. Images shown are representative of at least three independent experiments in each condition and were processed by using identical values for contrast and brightness.

RNA Isolation and Northern-Blot Analysis

Total RNA was isolated from cells treated for different times with 200 mM mannitol using Trizol reagent (Life Technologies, Mexico City) according to manufacturer's instructions. Typically, 200 mg of frozen cells were ground in a chilled mortar and suspended in 2 mL of Trizol reagent. After alcohol precipitation and washes, the RNA pellet was resuspended in diethyl pyrocarbonate-treated water, and LiCl was added to a final concentration of 1 M. Following centrifugation, the resulting RNA pellet was resuspended in diethyl pyrocarbonate-treated water and the amount of RNA was determined spectrophotometrically. Ten micrograms of purified total RNA was resolved on formaldehyde-agarose gels and transferred to Hybond-N+ nylon membrane (Amersham). Blots were screened with ^{32}P -labeled probes derived from *McTIP1;2* and *McHKT1* full-length cDNAs. After hybridization, blots were washed under high-stringency conditions (40 mM Na_2HPO_4 , pH 7.2, 1 mM EDTA, 1% SDS at 65°C) and subjected to autoradiography.

ACKNOWLEDGMENTS

We thank Drs. Ramon Serrano (Valencia, Spain), Phil Rea (Philadelphia), Karl-Josef Dietz (Bielefeld, Germany), and John C. Rogers (Pullman, WA) for antibodies against PMA1 (PM H^+ -ATPase), PAB-HK (vacuolar H^+ -pyrophosphatase), VMA-E (vacuolar H^+ -ATPase), and BP80, respectively, and Christophe Maurel for the *AtTIP1;1* construct. We also thank Enrique Balderas for help with the oocytes, Chris Michalowski for help with the cDNA constructs, and Xochitl Alvarado for help with the confocal microscope.

Received April 22, 2004; returned for revision May 31, 2004; accepted June 4, 2004.

LITERATURE CITED

- Aharon R, Shahak Y, Wininger S, Bendov R, Kapulnik Y, Galili G (2003) Overexpression of a plasma membrane aquaporin in transgenic tobacco improves plant vigor under favorable growth conditions but not under drought or salt stress. *Plant Cell* **15**: 439–447
- Barkla BJ, Vera-Estrella R, Maldonado-Gama M, Pantoja O (1999) Abscisic acid induction of vacuolar H^+ -ATPase activity in *Mesembryanthemum crystallinum* is developmentally regulated. *Plant Physiol* **120**: 811–819
- Baumgarten R, van de Pol MH, Wetzels JF, van Os CH, Deen PM (1998) Glycosylation is not essential for vasopressin-dependent routing of aquaporin-2 in transfected Madison-Darby canine kidney cells. *J Am Soc Nephrol* **9**: 1553–1559
- Bradford MM (1976) A rapid and sensitive method for the quantitation of microgram quantities of protein utilizing the principle of protein-dye binding. *Anal Biochem* **72**: 248–254
- Brown BE, Lemmon BE (1995) Methods in plant immunolight microscopy. In DW Galbraith, HJ Bohnert, DP Bourque, eds, *Methods in Plant Cell Biology*. Academic Press, New York, pp 85–107
- Brown D, Katsura T, Gustafson CE (1998) Cellular mechanisms of aquaporin trafficking. *Am J Physiol* **275**: F328–F331
- Cerioti A, Duranti M, Bollini R (1998) Effects of N-glycosylation on the folding and structure of plant proteins. *J Exp Bot* **49**: 1091–1103
- Chardin P, McCormick F (1999) Brefeldin A: the advantage of being uncompetitive. *Cell* **97**: 153–155
- Chaumont F, Barrieu F, Jung R, Chrispeels MJ (2000) Plasma membrane intrinsic proteins from maize cluster in two sequence subgroups with differential aquaporin activity. *Plant Physiol* **122**: 1025–1034
- Chaumont F, Barrieu F, Wojcik E, Chrispeels MJ, Jung R (2001) Aquaporins constitute a large and highly divergent protein family in maize. *Plant Physiol* **125**: 1206–1215
- Chrispeels MJ, Herman EM (2000) Endoplasmic reticulum-derived compartments function in storage and as mediators of vacuolar remodeling via a new type of organelle, precursor protease vesicles. *Plant Physiol* **123**: 1227–1233

- Dietz KJ, Arbinger B (1996) cDNA sequence and expression of subunit E of the vacuolar H⁺-ATPase in the inducible Crassulacean acid metabolism plant *Mesembryanthemum crystallinum*. *Biochim Biophys Acta* **1281**: 134–138
- Gomez L, Chrispeels MJ (1993) Tonoplast and soluble vacuolar proteins are targeted by different mechanisms. *Plant Cell* **5**: 1113–1124
- Hanoune J, Defer N (2001) Regulation and role of adenylyl cyclase isoforms. *Annu Rev Pharmacol Toxicol* **41**: 145–174
- Hazelton SR, Felgenhauer BE, Spring JH (2001) Ultrastructural changes in the Malpighian tubules of the House Cricket, *Acheta domesticus*, at the onset of diuresis: a time study. *J Morphol* **247**: 80–92
- Hodges TK, Leonard RT (1974) Purification of a plasma membrane-bound triphosphate from plant roots. *Methods Enzymol* **321**: 392–406
- Ishikawa Y, Skowronski MT, Inoue N, Ishida H (1999) α_1 -Adrenoceptor-induced trafficking of aquaporin-5 to the apical plasma membrane of rat parotid cells. *Biochem Biophys Res Commun* **265**: 94–100
- Jauh G-Y, Phillips TE, Rogers JC (1999) Tonoplast intrinsic protein isoforms as markers for vacuolar functions. *Plant Cell* **11**: 1867–1882
- Javot H, Lauvergeat V, Santoni V, Martin-Laurent F, Güçlü J, Vinh J, Heyes J, Franck KI, Schäffner AR, Bouchez D, et al (2003) Role of a single aquaporin isoform in root water uptake. *Plant Cell* **15**: 509–522
- Jiang L, Rogers JC (1998) Integral membrane protein sorting to vacuoles in plant cells: evidence for two pathways. *J Cell Biol* **30**: 1183–1199
- Kaldenhoff R, Grote K, Zhu J-J, Zimmermann U (1998) Significance of plasmalemma aquaporins for water-transport in *Arabidopsis thaliana*. *Plant J* **14**: 121–128
- Kim EJ, Zhen R-G, Rea PA (1994) Heterologous expression of plant vacuolar pyrophosphatase in yeast demonstrates sufficiency of the substrate-binding subunit for proton transport. *Proc Natl Acad Sci USA* **91**: 6128–6132
- Kirch H-H, Vera-Estrella R, Gollmack D, Quigley F, Michalowski CB, Barkla BJ, Bohnert HJ (2000) Expression of water channel proteins in *Mesembryanthemum crystallinum*. *Plant Physiol* **123**: 111–124
- Knepper MA, Inoue T (1997) Regulation of aquaporin-2 water channel trafficking by vasopressin. *Curr Opin Cell Biol* **9**: 560–564
- Laemmli UK (1970) Cleavage of structural proteins during assembly of the head of bacteriophage T4. *Nature* **227**: 680–685
- Lerouge P, Cabanes-Macheteau M, Rayon C, Fischette-Lairé AC, Gomord V, Faye L (1998) N-glycoprotein biosynthesis in plants: recent developments and future trends. *Plant Mol Biol* **38**: 31–48
- Liu LH, Ludewig U, Gasset B, Frommer WB, Von Wirén N (2003) Urea transport by nitrogen-regulated tonoplast intrinsic proteins in *Arabidopsis*. *Plant Physiol* **133**: 1220–1228
- Manolson ME, Rea PA, Poole RJ (1985) Identification of 3-O-(4-benzoyl)benzoyladenine 5'-triphosphate- and N,N'-dicyclohexylcarbodiimide-binding subunits of a higher plant H⁺-translocating tonoplast ATPase. *J Biol Chem* **260**: 12273–12279
- Martre P, Morillon R, Barrieu F, North GB, Nobel PS, Chrispeels MJ (2002) Plasma membrane aquaporins play a significant role during recovery from water deficit. *Plant Physiol* **130**: 2101–2110
- Marty F (1999) Plant vacuoles. *Plant Cell* **11**: 587–599
- Matsuoka K, Bassham DC, Raikhel NV, Nakamura K (1995) Different sensitivity to wortmannin of two vacuolar sorting signals indicates the presence of distinct sorting machineries in tobacco cells. *J Cell Biol* **130**: 1307–1318
- Maurel C, Javot H, Lauvergeat V, Gerbeau P, Tournaire C, Santoni V, Heyes J (2002) Molecular physiology of aquaporins in plants. *Int Rev Cytol* **215**: 105–148
- Maurel C, Kado RT, Guern J, Chrispeels MJ (1995) Phosphorylation regulates the water channel activity of the seed-specific aquaporin α -TIP. *EMBO J* **14**: 3028–3035
- Maurel C, Reizer J, Schroeder JI, Chrispeels MJ (1993) The vacuolar membrane protein α -TIP creates water specific channels in *Xenopus* oocytes. *EMBO J* **12**: 2241–2247
- Moutinho A, Hussey PJ, Trewavas AJ, Malhó R (2001) cAMP acts as a second messenger in pollen tube growth and reorientation. *Proc Natl Acad Sci USA* **98**: 10481–10486
- Murashige T, Skoog F (1962) A revised medium for rapid growth and bioassay with tobacco tissue cultures. *Physiol Plant* **15**: 473–479
- Nelson DE, Glaunsinger B, Bohnert HJ (1997) Abundant accumulation of the calcium-binding molecular chaperone calreticulin in specific floral tissues of *Arabidopsis thaliana*. *Plant Physiol* **114**: 29–37
- Newton RP, Roef L, Witters E, Van Onckelen H (1999) Cyclic nucleotides in higher plants: the enduring paradox. *New Phytol* **143**: 427–455
- Nielsen S, Chou CL, Marples D, Christensen EI, Kishore BK, Knepper MA (1995) Vasopressin increases water permeability of kidney collecting duct by inducing translocation of aquaporin-CD water channels to plasma membrane. *Proc Natl Acad Sci USA* **92**: 1013–1017
- Pardo JM, Serrano R (1989) Structure of a plasma membrane H⁺-ATPase gene from the plant *Arabidopsis thaliana*. *J Biol Chem* **264**: 8557–8562
- Paris N, Rogers SW, Jiang L, Kirsch T, Beevers L, Phillips TE, Rogers JC (1997) Molecular cloning and further characterization of a probable plant vacuolar sorting receptor. *Plant Physiol* **115**: 29–39
- Paris N, Stanley CM, Jones RL, Rogers JC (1996) Plant cells contain two functionally distinct vacuolar compartments. *Cell* **85**: 563–572
- Parry RV, Turner JC, Rea PA (1989) High purity preparations of higher plant vacuolar H⁺-ATPase reveal additional subunits: revised subunit composition. *J Biol Chem* **264**: 20025–20032
- Quigley F, Rosenberg JM, Shachar-Hill Y, Bohnert HJ (2002) From genome to function: the *Arabidopsis* aquaporins. *Genome Biol* **3**: 1–17
- Ritzenthaler C, Nebenführ A, Movafeghi A, Stussi-Garud C, Behnia L, Pimpl P, Staehelin LA, Robinson DG (2002) Reevaluation of the effects of brefeldin A on plant cells using tobacco bright yellow 2 cells expressing Golgi-targeted green fluorescent protein and COP1 antisera. *Plant Cell* **14**: 237–261
- Robinson DG, Sieber H, Kammerloher W, Schäffner AR (1996) PIP1 aquaporins are concentrated in plasmalemmasomes of *Arabidopsis* mesophyll. *Plant Physiol* **111**: 645–649
- Sanderfoot AA, Ahmed SU, Marty-Mazars D, Rapoport I, Kirchhausen T, Marty F, Raikhel NV (1998) A putative vacuolar cargo receptor partially colocalizes with AtPEP12p on a prevacuolar compartment in *Arabidopsis* roots. *Proc Natl Acad Sci USA* **95**: 9920–9925
- Santoni V, Gerbeau P, Javot H, Maurel C (2000) The high diversity of aquaporins reveals novel facets of plant membrane functions. *Curr Opin Plant Biol* **3**: 476–481
- Siefritz F, Tyree MT, Lovisolo C, Schubert A, Kaldenhoff R (2002) PIP1 plasma membrane aquaporins in tobacco: from cellular effects to function in plants. *Plant Cell* **14**: 869–876
- Simonsen A, Wurmser AE, Emr SD, Stenmark H (2001) The role of phosphoinositides in membrane transport. *Curr Opin Cell Biol* **13**: 485–492
- Sparvoli F, Faoro F, Daminati MG, Ceriotti A, Bollini R (2000) Misfolding and aggregation of vacuolar glycoproteins in plant cells. *Plant J* **24**: 825–836
- Tyerman SD, Bohnert HJ, Maurel C, Steudle E, Smith JAC (1999) Plant aquaporins: their molecular biology, biophysics and significance for plant water relations. *J Exp Bot* **50**: 1055–1071
- Tyerman SD, Niemietz CM, Bramley H (2002) Plant aquaporins: multifunctional water and solute channels with expanding roles. *Plant Cell Environ* **25**: 173–194
- Uehlein N, Lovisolo C, Siefritz F, Kaldenhoff R (2003) The tobacco aquaporin *NtAQP1* is a membrane CO₂ pore with physiological functions. *Nature* **16**: 734–738
- Vera-Estrella R, Barkla BJ, Bohnert HJ, Pantoja O (1999) Salt stress in *Mesembryanthemum crystallinum* L. cell suspensions activates adaptive mechanisms similar to those observed in the whole plant. *Planta* **207**: 426–435
- Vera-Estrella R, Barkla BJ, Gallardo-Amarillas C, Bohnert HJ, Pantoja O (2000) Aquaporin regulation under salt and osmotic stress in the halophyte *Mesembryanthemum crystallinum* L. In S Hohmann, S Nielsen, eds, *Molecular Biology and Physiology of Water and Solute Transport*. Kluwer Academic/Plenum Publishers, New York, pp 339–346
- Wayne R, Tazawa M (1988) The actin cytoskeleton and polar water permeability in Characean cells. *Protoplasma Suppl* **2**: 116–130
- Woscholski R, Kodaki T, McKinnon M, Waterfield MD, Parker PJ (1994) A comparison of demethoxyviridin and wortmannin as inhibitors of phosphatidylinositol 3-kinase. *FEBS Lett* **342**: 109–114